Specific heat, thermal diffusivity, and thermal conductivity of FeF_2 at the Néel temperature

M. Marinelli and F. Mercuri
Dipartimento di Ingegneria Meccanica, II Università di Roma "Tor Vergata," Via della Ricerca Scientifica, 00133 Roma, Italy

D. P. Belanger
Physics Department, University of California, Santa Cruz, California 95064
(Received 13 July 1994; revised manuscript received 24 October 1994)

Photopyroelectric simultaneous measurements of the specific heat, thermal diffusivity, and thermal conductivity of single-crystalline FeF_2 at the antiferromagnetic-paramagnetic phase transition have been performed. An Ising-like behavior has been found for the specific heat for $|t| \leq 1.2 \times 10^{-2}$, while, in the same reduced-temperature range, the thermal-diffusivity critical behavior has been described according to a dynamic model for a uniaxial system with energy conservation with a critical exponent $b = -0.11 \pm 0.02$. No clear power-law anomaly has been found in the thermal conductivity.

INTRODUCTION

The static critical behavior of uniaxial magnetic systems has been widely studied in the past. Very many experimental results confirm the theoretical predictions based on the Ising model. Critical dynamics, on the other hand, is, generally speaking, somewhat less well established, both from the theoretical and experimental point of view. In the case of uniaxial systems, for example, two different models have been suggested:[1] model A in which the order parameter and the energy are nonconserved quantities and model C where the energy is conserved but the order parameter is not. In the case of uniaxial antiferromagnets, where the order parameter is the staggered magnetization, which is not conserved, the more appropriate model depends on the rate of energy transfer from the spin system to the phonons. If this process is slow then model C seems to be more appropriate, otherwise model A should be considered. Moreover, the predictions[1] for the dynamic critical exponent z resulting from these two models are connected to static exponents by the scaling laws $z = 2 + c\eta$ for model A and $z = 2 + \alpha/\nu$ for model C. Since $\alpha/\nu \sim 0.17$ and $c\eta \sim 0.02$ this results in a very small deviation from the $z = 2$ value which is expected for the conventional van Hove theory.[1] If critical dynamics is investigated through the study of thermal transport properties, such as the thermal conductivity (k) and the thermal diffusivity ($D = k/\rho c$, where ρ is the density and c is the specific heat), the situation is even more complicated due to some experimental difficulties. High-resolution measurements are needed, of course, and this essentially means that thermal gradients in the sample should be as small as possible. This is in conflict with the intrinsic need of thermal gradients in a thermal transport measurement.

A photopyroelectric technique has been recently used to simultaneously investigate the critical behavior of specific heat, thermal diffusivity, and thermal conductivity of Cr_2O_3 at the antiferromagnetic-paramagnetic (AF) phase transition.[2] It has been shown that if $|t| = |T - T_N|/T_N < 10^{-3}$ the critical behavior of the thermal diffusivity can be explained in terms of model C. It has also been shown that in the same reduced-temperature range the critical exponent for the specific heat is $\alpha = 0.10 \pm 0.02$ which agrees with the Ising prediction. Cr_2O_3 is a weakly anisotropic system and this is the reason why the above-mentioned behavior could be found only in a very narrow reduced-temperature range around T_N. It would be therefore very interesting to see if the same conclusions can be drawn for a strongly anisotropic system whose static critical behavior can be clearly described in terms of the Ising model.

In the present paper, high-resolution simultaneous measurements of the specific heat, thermal diffusivity, and thermal conductivity of FeF_2 in the vicinity of the Néel temperature are reported. FeF_2 is a well known, strongly anisotropic antiferromagnet whose static critical behavior can be well described by the Ising model.[3] It should be pointed out that the possibility of a simultaneous measurement of both static and dynamic quantities on the same sample under the same experimental conditions, such as thermal gradients, heating rate, etc., can greatly help when using the results of the measurements in scaling laws. It will be shown that the thermal diffusivity shows a dip at T_N due to the critical slowing down, which can be interpreted in terms of the above-mentioned model C, in the same reduced temperature range where the specific heat shows a clear Ising-like behavior. Data on the thermal conductivity are also reported.

FeF_2 PROPERTIES

FeF_2 is a well-characterized insulating two-sublattice antiferromagnet with a large anisotropy, making it an ideal system for the study of the Ising model. The magnetic Fe^{++} ions form a body-centered tetragonal lattice and interact through the fluorine superexchange interaction. With no field or stress applied, the two sublattices are magnetically equivalent. The magnetic interactions

0163-1829/95/51(14)/8897(7)/$06.00

can be well described by the Hamiltonian[4]

$$H = J \sum_{\langle i,j \rangle} \bar{S}_i \cdot \bar{S}_j - G \sum_i S_i^{z^2} , \quad (1)$$

where only next-nearest-neighbor interactions, $J = 0.435$ meV, between the body-center and body corner ions are included and $G = 0.861$ meV. All other exchange interactions are negligible. The uniaxial anisotropy is largely single ion in nature and is large enough such that the asymptotic Ising power-law behavior is observed for reduced temperature $|t| < 2 \times 10^{-2}$ in experimental critical behavior experiments.

The sample used in the present experiments is a single crystal grown using the Bridgman technique and has lattice parameters $a = b = 4.70$ Å and $c = 3.31$ Å. A single-crystal plate of 1 cm diameter was cut and polished to a finished thickness of 620 μm with the c axis perpendicular to the faces of the plate.

The static critical behavior of this system has been determined through a comprehensive series of experiments. The specific heat has been measured using adiabatic heat pulse techniques and optical linear birefringence.[3] The staggered susceptibility and correlation length have been determined using quasielastic neutron-scattering techniques.[5] The critical behavior of the staggered magnetization has been determined using Mössbauer techniques.[6] All of these results have been summarized,[7] along with the corresponding theories. The agreement between all of the experimentally and theoretically determined universal exponents and amplitude ratios is exceedingly good.

The dynamic critical behavior has been investigated[8] using spin-echo neutron scattering. The result $z = 2.0 \pm 0.1$ is not particularly enlightening with regard to distinguishing between models A and C since the predicted exponents of both models fall within the experimental error estimates. The present pyroelectric technique, on the other hand, does have the capability to make that distinction.

EXPERIMENT

The photopyroelectric technique is based on the pyroelectric detection of temperature oscillations introduced in a sample by a modulated heating source.[9] In the so-called back detection configuration, the sample, which is usually a thin slab, is heated on one side and the temperature oscillations are detected on the opposite side. In the present work, one surface of the 620-μm-thick FeF_2 was in thermal contact, by means of a very thin, thermally transparent, silicone grease layer, with a 300-μm-thick $LiTaO_3$ pyroelectric single crystal. To heat the sample on the opposite side, we used a 633-nm, 10-mW He-Ne laser beam acousto-optically modulated at $f = 78$ Hz. Since FeF_2 is transparent in the visible, we coated that surface with a 200-nm Ti overlayer. As will be shown later on, the effect of the silicone grease and that of the metallic coating on the heat transport process is negligible. It has been shown that in a one-dimensional heat flow process, if the sample and the transducer are optically opaque and thermally thick, c, k, and D can be simultaneously measured,[10] provided that the sample density ρ and the transducer properties are known. As a matter of fact, only two of these quantities, usually D and c, can be obtained from the measurements while the third one is calculated from $D = k/\rho c$. The FeF_2 density is well behaved near T_N and it decreases by only 0.4% from room temperature to liquid-helium temperature.[11]

The sample and the transducer were contained in a variable temperature cryostat and the light intensity impinging on the sample was controlled by means of a negative lens. It is known that too fast a heating rate and too high a power density can decrease the resolution of the measurements, the sample not being in thermal equilibrium. We successively decreased the power density and the heating rate to values where a further decrease gave no effect on the experimental resolution. The temperature rate change we used was (10 ± 1) mK/min and the data were collected every 3 mK. The use of the negative lens also ensures the one-dimensional geometry of the heat flow in the system, since the dimension of the illuminated area was much greater than the sample thickness. We also made some measurements at frequencies other than 78 Hz but the results we obtained for the thermal parameters did not show any significant change, thus making sure that there is no contribution in the heat transport process coming from the Ti coating and the coupling fluid.

As stated before, the simultaneous determination of c, k, and D is possible only under certain experimental conditions. In particular if the sample and the pyroelectric are thermally thick ($\mu_s \ll l_s$ and $\mu_p \ll l_p$ where $\mu = \sqrt{D/\pi f}$ is the heat diffusion length, l is the thickness, f is the modulation frequency, and subscripts s and p refer to the sample and the transducer, respectively), the sample is optically opaque ($\mu_\beta \ll l_s$ where μ_β is the optical penetration depth) and the optical penetration depth is much smaller than the heat diffusion length ($\mu_\beta \ll \mu_s$), then the photopyroelectric signal amplitude and phase are

$$|V| \propto \frac{1}{\sqrt{1+(2\pi f \tau_e)^2}} \frac{e^{-\sqrt{\pi f/D} l_s}}{(e_s/e_p + 1)} , \quad (2)$$

$$\phi = -\arctan(2\pi f \tau_e) - \sqrt{\pi f/D} l_s , \quad (3)$$

where the $f_e = 1/2\pi\tau_e$ is the transducer plus detection electronic cutoff frequency, $e = \sqrt{\rho c k}$ is the thermal effusivity. The thermal diffusivity can be calculated from the signal phase and then submitted in the signal amplitude to obtain the sample thermal effusivity. Specific heat and thermal conductivity can be calculated as follows:

$$c_s = e_s/\rho_s \sqrt{D_s}, \quad k_s = e_s \sqrt{D_s}$$

if ρ_s and e_p are known and constant.

Provided that $2\pi f \tau_e \gg 1$, Eqs. (2) and (3) can be rewritten as $\ln(fx|V|) \propto -(\sqrt{\pi/D}\, l_s)\sqrt{f}$ and $\phi \propto -(\sqrt{\pi/D}\, l_s)\sqrt{f}$, respectively. It can be seen that if the conditions for which these two expressions have been obtained are valid then the plots of $\ln(fx|V|)$ and ϕ as a function of $\sqrt{f}$ must give two straight lines with the

same slope. Moreover from the slope an absolute value of the sample thermal diffusivity can be obtained once l_s is known. Figure 1 shows the results of a frequency scan made at 87.85 K where a linear dependence in the frequency range 30–200 Hz can be easily seen. The 78-Hz frequency we have chosen in our experiment is well within that linear region thus confirming that a simultaneous determination of c, k, and D is possible. It should also be noted that the slopes we have obtained are the same, thus giving one more experimental evidence that the results are not affected by the presence of the coating and the silicone grease. We obtained $D=(0.196\pm0.016)$ cm^2/s. A normalization for the amplitude and phase has been performed using the data reported in Ref. 3 for the specific heat at $T=87.85$ K, which is a temperature far away from the transition temperature. We have also used for the normalization the absolute value for the thermal diffusivity we have measured at the same temperature with a frequency scan. The normalization is necessary to make sure that the results are only dependent on the sample parameters. The normalization temperature has been chosen sufficiently away from the transition temperature to make sure that possible differences in purity and homogeneity between our sample and that of Ref. 3 are not relevant.

EXPERIMENTAL RESULTS

Figure 2 shows the results we have obtained for the specific heat in the temperature range 72–90 K, compared with some selected data points taken from Ref. 3. The normalization has been done at $T=87.85$ K using one data point taken from Ref. 3, but the two curves superimpose quite well over the whole temperature range. This comparison gives an indication of the quality of the measurement which is of course applicable to dynamic quantities also since they are measured simultaneously. As stated before we have also performed measurements at different frequencies, but the data we obtained did not show any significant difference with respect to the ones reported in Fig. 2.

The thermal conductivity data, reported in Fig. 3,

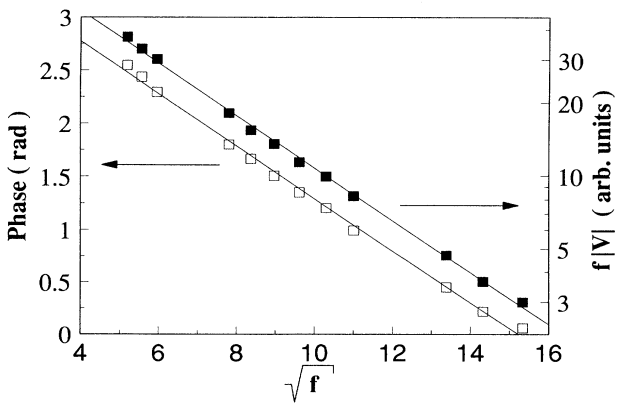

FIG. 1. Photopyroelectric phase (□) and frequency-amplitude product (■) vs the square root of the modulation frequency.

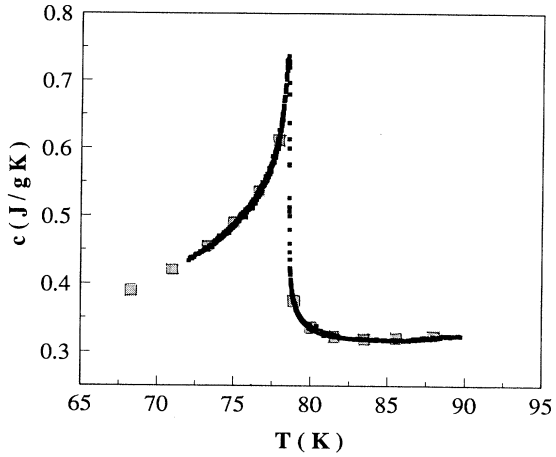

FIG. 2. Specific-heat data as a function of temperature. (▨) are specific-heat data taken from Ref. 3.

show a very broad peak around T_N with some additional features at T_N. In particular, a slight decrease is evident on the low temperature side of T_N, while there is an increase close to T_N as shown in the inset of Fig. 3.

Figure 4 shows the thermal diffusivity data where a dip, due to the critical slowing down, is clearly evident near T_N. A similar behavior has been reported for the AF transition in Cr_2O_3.

DATA ANALYSIS: FITTING FUNCTIONS

To fit the specific-heat data we have used the following fitting function:

$$C_p = A|T-T_N|^{-\alpha}(1+D|T-T_N|^{0.5})+B+E(T-T_N)\ , \tag{4}$$

where α, A, B, D, and E are adjustable parameters and, as usual, primed parameters will be used for $T<T_N$. The

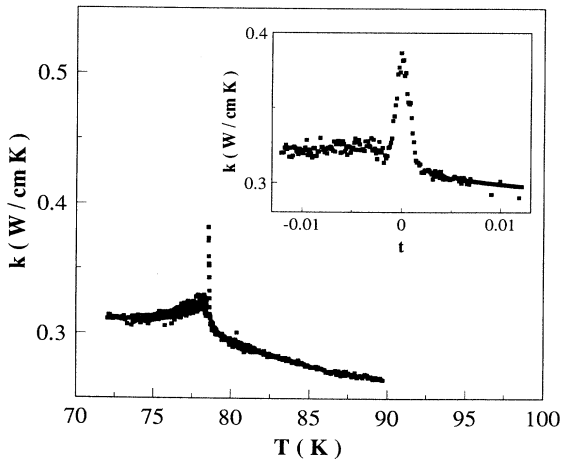

FIG. 3. Thermal conductivity data as a function of temperature. k data as a function of the reduced temperature in the vicinity of the transition temperature are reported in the inset.

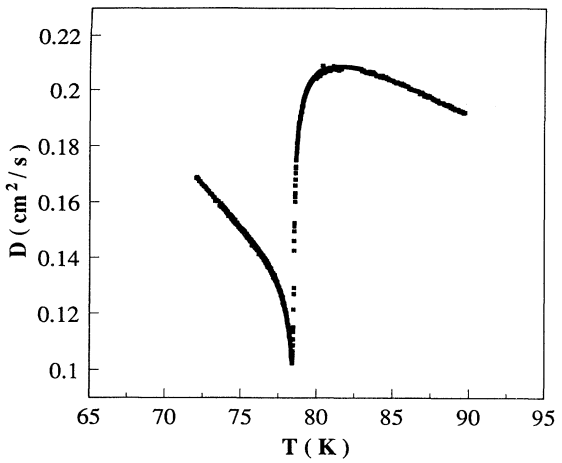

FIG. 4. Thermal diffusivity data as a function of temperature.

linear term represents a nonsingular contribution to the specific heat and we therefore expect $E=E'$. We also know that $\alpha=\alpha'$. The fitting procedure is the same that has been used in Ref. 2. Data have been fitted with a nonlinear least-squares routine, initially assuming $D=D'=0$, $B=B'$, $\alpha=\alpha'$, and $E=E'$. After first roughly estimating data which are affected by rounding and eliminating them, we fit the remaining data. Next, we included more and more data points nearer to T_N, which did not affect the fit quality. For every fit we considered not only the rms value but also the deviation plot. After this, all the constraints were released and the data fitted again. Finally we allowed a nonzero value for D and D'. The function we minimize is a χ^2-like function and the uncertainty in the case of the specific heat was 0.08% while in the case of the thermal diffusivity was 0.03%. For the thermal diffusivity we used a similar expression with a regular term plus a singular one, with a correction term:

$$D=U|T-T_N|^{-b}(1+F|T-T_N|^{0.5}) + V+W(T-T_N) \quad (\text{with } b<0)\ . \tag{5}$$

The constraint on b is due to the fact that D, which in our case decreases, cannot go to minus infinity at T_N. The correction term we have used is similar to the one which has been used in Ref. 2.

RESULTS

The results for the specific heat are reported in Table I. Fit 1 has been obtained with $D=D'=0$. The values of the critical exponent $\alpha=0.10\pm0.02$ and of $A/A'=0.53\pm0.08$ seem to agree quite well with the prediction of the Ising model[12] ($\alpha=0.110\pm0.0045$ and $A/A'=0.51$) and previous experimental results.[7] It is not clear why we have smaller $t_{\min}$ values for $T>T_N$ with respect to the ones for $T<T_N$, but it could be due to some rounding effects introduced by residual thermal gradients in the sample. Fit 2 has been performed with $D\neq D'\neq 0$ in approximately the same reduced temperature range of fit 1 and the results, as far as the critical exponent and the critical amplitude ratio are concerned, are again in very good agreement with the Ising-like model predictions. The deviation plot reported in Fig. 5(a), which is very similar to the one of fit 1 (not shown), appears to show a good fit quality. On the other hand, the ratio $D/D'=-0.4$ does not agree with the prediction $D/D'\sim 1$ for the Ising model.[13] This disagreement can be explained if the statistical errors corresponding to D are considered. Let us remember that the statistical error is defined as the variation of the fitting parameter which causes a variation of one standard deviation in the function which has to be minimized, adjusting all the other parameters. The rather poor influence that D has on the fit quality is reflected in the large estimated error. Fit 2 seems moreover to have problems as far as the E parameter is concerned. A value of $E\sim 2\times10^{-3}$ can be obtained considering high-temperature c data reported in Fig. 2, which can be described by the expression $B+E(T-T_N)$. It should be noted however that the difference between the value obtained from the fit and the one obtained from the figure is within the statistical error. As a check we tried to fit the data with $E=2\times10^{-3}$ fixed and the constraint $D=D'$. Fit 3 shows the results which have been obtained and the deviation plot is reported in Fig. 5(b). The fit quality is very good and no

TABLE I. Results of the fits for the specific heat.

	Fit 1	Fit 2	Fit 3	Fit 4
$t_{\max}$	1.2×10^{-2}	1.2×10^{-2}	1.2×10^{-2}	8.0×10^{-3}
$t_{\min}$ ($T<T_c$)	1.6×10^{-3}	1.5×10^{-3}	1.6×10^{-3}	1.5×10^{-3}
$t_{\min}$ ($T>T_c$)	6.9×10^{-5}	6×10^{-5}	8×10^{-5}	8×10^{-5}
T_c (K)	78.56±0.02	78.55±0.02	78.56±0.02	78.55±0.02
α	0.10±0.02	0.11±0.03	0.10±0.03	0.11±0.03
A' (J/gK)	$(6.0\pm0.4)\times10^{-1}$	$(5.8\pm0.3)\times10^{-1}$	$(5.4\pm0.4)\times10^{-1}$	$(5.8\pm0.3)\times10^{-1}$
A (J/gK)	$(3.2\pm0.3)\times10^{-1}$	$(3.2\pm0.2)\times10^{-1}$	$(2.7\pm0.3)\times10^{-1}$	$(3.4\pm0.3)\times10^{-1}$
E (J/gK)	$(2\pm2)\times10^{-2}$	$(2\pm2)\times10^{-2}$	2×10^{-3}	$(6\pm4)\times10^{-2}$
B (J/gK)	$(1.1\pm0.9)\times10^{-4}$	$(5\pm7)\times10^{-4}$	$(7\pm3)\times10^{-2}$	$(5\pm3)\times10^{-3}$
D'		$(5\pm4)\times10^{-2}$	$(-4\pm3)\times10^{-2}$	$(6\pm3)\times10^{-2}$
D		$(-2\pm4)\times10^{-2}$	$(-4\pm3)\times10^{-2}$	$(-2\pm1)\times10^{-1}$
A/A^-	0.53±0.08	0.55±0.06	0.50±0.09	0.57±0.08
rms	0.0090	0.0089	0.01	0.0097

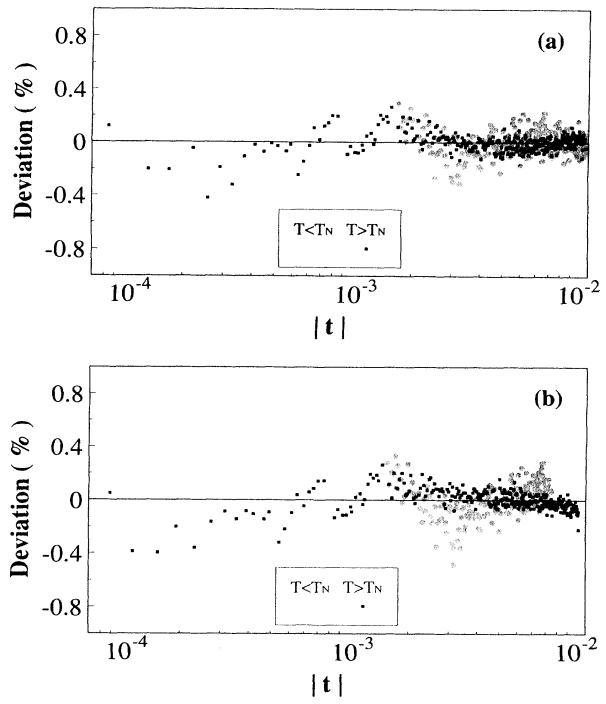

FIG. 5. Deviation plots corresponding to fits of Table I: (a) fit 2, (b) fit 3.

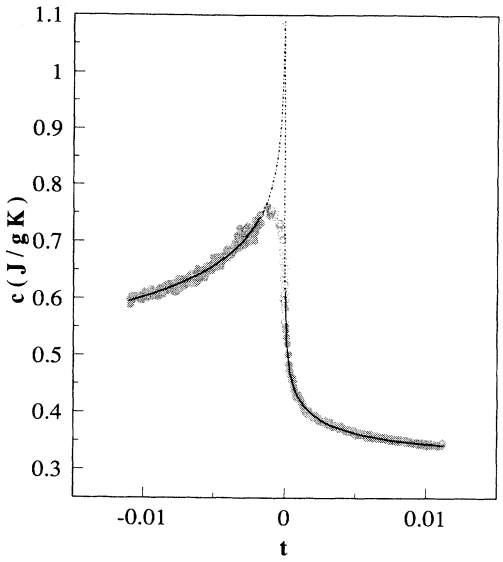

FIG. 6. Specific-heat data vs reduced temperature. Symbols are much larger than the experimental uncertainties (see text). The solid line corresponds to fit 2 of Table I. The dotted line corresponds to the reduced temperature region which has not been considered in the fit.

significant changes can be detected for α and for the critical amplitudes with respect to fits 1 and 2. As a conclusion we can say that even if the Ising-like behavior seems to be confirmed, the data do not allow any conclusion on the D/D' ratio. Moreover the E and B parameters seem not to affect significantly the fit in the reduced temperature range we have considered. The statistical errors on these terms can be decreased if a wider temperature range is considered, but in this case an increase in error on α and A is observed. We have also tried a range of reduced temperature closer to T_N to see if this affects the critical exponent and the fitting parameters. The results correspond to fit 4 where no significant change can be detected with respect to fit 3. It should be noted that the number of data points included in fits 1, 2, and 3 are more than 550. Figure 6 shows the specific-heat data together with the best-fit curve corresponding to fit 2.

The results for the thermal diffusivity are reported in Table II. Again fit 5 has been obtained putting $F=F'=0$. The critical exponent $b=-0.09\pm0.03$ and the critical amplitude ratio $U/U'=1.74\pm0.08$ are quite close to the values of -0.09 ± 0.01 and 1.95 ± 0.08 obtained for the thermal diffusivity of Cr_2O_3 in the reduced temperature range where the data could be described in terms of model C. The fit quality seems to be quite good as it turns out from the deviation plot (not shown). Fit 6 has been obtained with $F\neq F'\neq 0$ and the corresponding deviation plot is shown in Fig. 7(a). This fit has a smaller

TABLE II. Results of the fits for the thermal diffusivity.

	Fit 5	Fit 6	Fit 7	Fit 8
t_{max}	1.2×10^{-2}	1.2×10^{-2}	1.2×10^{-2}	8.0×10^{-3}
t_{min} $(T<T_c)$	1.3×10^{-3}	1.5×10^{-3}	1.3×10^{-3}	1.4×10^{-3}
t_{min} $(T>T_c)$	2.6×10^{-4}	1.2×10^{-4}	3×10^{-4}	2.0×10^{-4}
T_c (K)	78.52±0.02	78.53±0.02	78.51±0.02	78.53±0.02
b	−0.09±0.03	−0.11±0.02	−0.11±0.04	−0.11±0.02
U' (cm²/s)	$(1.21\pm0.04)\times10^{-1}$	$(1.15\pm0.03)\times10^{-1}$	$(1.31\pm0.04)\times10^{-1}$	$(1.14\pm0.03)\times10^{-1}$
U (cm²/s)	$(2.10\pm0.04)\times10^{-1}$	$(2.25\pm0.04)\times10^{-1}$	$(2.25\pm0.04)\times10^{-1}$	$(2.25\pm0.04)\times10^{-1}$
W (cm²/s)	$(-8.5\pm0.9)\times10^{-3}$	$(1.2\pm0.6)\times10^{-2}$	$(-8.0\pm0.8)\times10^{-3}$	$(1.1\pm0.7)\times10^{-2}$
V (cm²/s)	$(5\pm5)\times10^{-4}$	$(5\pm8)\times10^{-3}$	$(1\pm2)\times10^{-4}$	$(5\pm7)\times10^{-3}$
F'		$(2\pm4)\times10^{-1}$	$(-7\pm6)\times10^{-2}$	$(2\pm3)\times10^{-1}$
F		$(-2\pm3)\times10^{-1}$	$(-7\pm6)\times10^{-2}$	$(-2\pm2)\times10^{-1}$
U/U'	1.74±0.08	1.97±0.08	1.72±0.08	1.97±0.08
rms	0.0050	0.0036	0.0044	0.0043

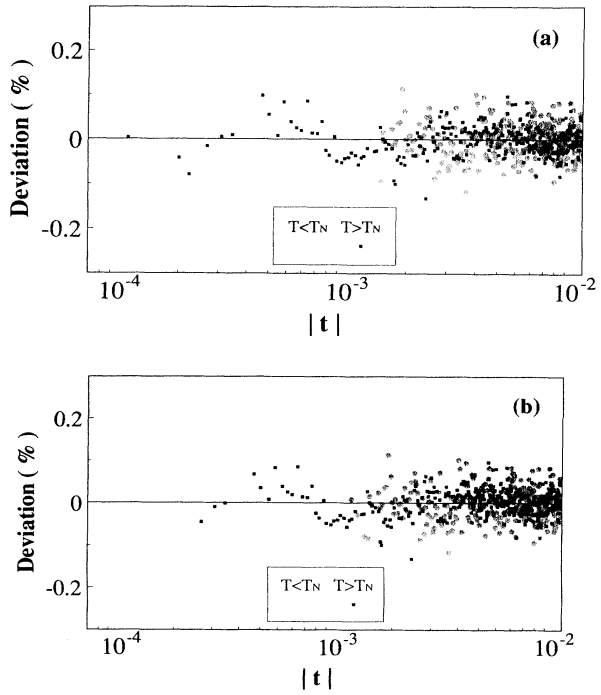

FIG. 7. Deviation plots corresponding to fits of Table II: (a) fit 6, (b) fit 7.

rms value and shows a slight improvement in the deviation plot. We obtained $b=-0.11\pm0.02$ and $U/U'=1.97\pm0.08$. Also in this case we obtained F and F' which are opposite in sign. Although there are no theoretical predictions on the ratio F/F', since we have found a rather constant thermal conductivity, we should expect $F/F'\sim 1$ as in the case of the D parameter in the specific heat. Also in this case the statistical errors on F and F' are large and we therefore tried to fit the data with the constraint $F=F'$. Fit 7 shows the results obtained: the deviation plot [Fig. 7(b)] and the rms value tell us that the fit quality is very close to the one of fit 6 and no significant variations of b and U/U' can be detected. Again the data in the reduced temperature we have considered in the fit do not allow any conclusion on the ratio F/F'. Also in this case we tried to reduce the fitting interval but no significant change can be obtained as shown in fit 8. Figure 8 shows the thermal diffusivity data with the best-fit curve corresponding to fit 5.

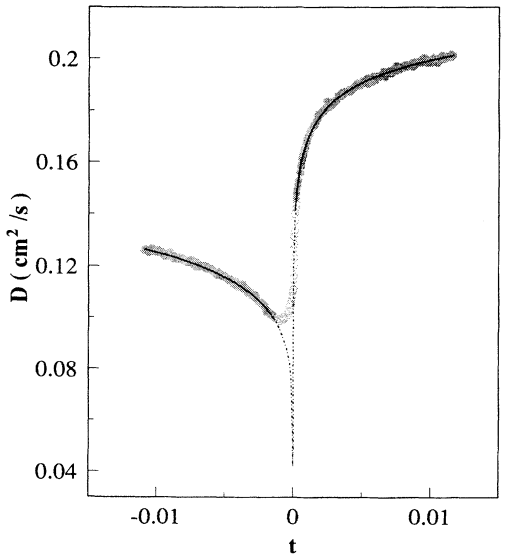

FIG. 8. Thermal-diffusivity data vs reduced temperature. Symbols are much larger than the experimental uncertainties (see text). The solid line corresponds to fit 6 of Table II. The dotted line corresponds to the reduced temperature region which has not been considered in the fit.

DISCUSSION

The specific-heat data confirm the Ising-like behavior of FeF_2 at the AF transition as previously reported by several authors. These data can be used as a check on the reliability of the measurements. It should be noted that, while the thermal diffusivity is derived from the phase of the photopyroelectric signal, the specific heat is obtained by considering both the amplitude and phase, thus being affected by the uncertainties of both. Hence, if the c data are reliable, the D data must be even more reliable.

The fits of the thermal diffusivity data give results that are very similar to the ones which have been obtained for Cr_2O_3 for $|t|<10^{-3}$. For that material, due to its very weak anisotropy, a crossover behavior was found if wider reduced temperature ranges were considered. In the present case approximately the same power-law behavior has been obtained for $|t|<1.2\times10^{-2}$. FeF_2 is a strongly anisotropic uniaxial material which can be considered a more ideal Ising-like system. The energy of the spin system can or cannot be the only conserved quantity, since the staggered magnetization, which is the order parameter, is not conserved. As already stated the energy conservation depends on the rate of energy transfer from the spin system to the phonons: if this process is slow, the spin system can be considered isolated, the energy is conserved, and the critical dynamics can be described in terms of the model C; if the transfer is not relatively slow, model A should be more appropriate.

Assuming that the dynamic scaling hypothesis is applicable to the energy (extended scaling[14]), it has been shown[1] for model C that $\omega_E=iDq^2\propto q^{z_E}$, where q is the mode wave vector, $z_E=2+\tilde{\alpha}/\nu$ and $\tilde{\alpha}=\max(\alpha,0)$. If the energy is conserved we have only purely diffusive heat conduction modes[1] and, since $D\propto|T-T_c|^{-b}$, we obtain $\omega_E=iDq^2\propto\xi^{b/\nu}q^2=(q\xi)^{b/\nu}q^{2-b/\nu}$, where ξ is the correlation length and therefore $z_E=2-b/\nu$. We therefore expect for model C that $-b=\alpha$ and this is what we obtained from the fits. This means that the heat conduction mode does not couple with the order-parameter mode. These conclusions are the same conclusions which have been drawn for the Cr_2O_3 in a very narrow reduced temperature range around T_N. In that case, however, the situation was more complicated since a crossover behavior was obtained for a wider reduced temperature range. This was also confirmed by the specific-heat data which show in the same narrow reduced temperature range an Ising-like behavior and a crossover on a wider t range. In

the present case the conclusion is somewhat less ambiguous since, as stated before, FeF_2 is an ideal Ising-like system. We would like to stress that approximately the same value for U/U' has been obtained for the two systems. As far as we know, no universal predictions are available in literature for this quantity. However, if $b=-\alpha$, it is not unlikely that $A/A' \approx U'/U$, and this is certainly within the fitting error of these two ratios.

Whereas the diffusivity and the specific heat appear to have the same critical exponent, it is clearly evident in Fig. 3 that the thermal conductivity has a broad peak with some additional features superimposed at T_N. The critical exponent of the thermal conductivity has been generally derived in theoretical works[15] considering only the singular terms of the thermal diffusivity and of the specific heat. This approach seems not to be correct because the critical behavior of these two quantities is described not only by the singular terms but also by regular terms as shown in Eqs. (5) and (4). It seems more correct in deriving the critical exponent of the thermal conductivity from the specific heat and from the diffusivity to consider the whole expression for their critical behavior. This explains the small anomaly background seen in Fig. 3, but does not explain the large spike very close to T_N, nor the slight dip just below T_N. The latter features only occur approximately for $|t|<10^{-3}$ and we believe are attributable to thermal gradients which occur at this level. If $b=-\alpha$, the power-law behaviors cancel everywhere except in the region where thermal gradients occur. The failure of the power-law cancellation results in the spike observed. Assuming that the influence of the gradients for D is slightly smaller than for c, the downward deflection below T_N will occur. Finally, unless $A/A' \approx U'/U$, the simulation indicates a large step at T_N. Indeed no large step is indicated by the data. All of these conclusions are supported by qualitative computer simulations of the effects of gradients on the conductivity similar to those reported for the specific heat alone.[16]

CONCLUSIONS

A photopyroelectric technique has been used to simultaneously measure the specific heat, thermal diffusivity, and thermal conductivity critical behavior of FeF_2 in the vicinity of the Néel temperature. Specific-heat data are in agreement with the ones previously reported and show, as expected, an Ising-like behavior. The thermal diffusivity data can be explained in terms of a dynamic model (model C) for uniaxial systems with energy conservation for the spin system. We obtained for the diffusivity critical exponent $b=-0.11\pm0.02$ which satisfy the scaling law $-b=\alpha$ which is valid for the abovementioned model. The thermal conductivity data show a broad peak with some structures in the vicinity of the transition but no clear anomaly has been detected.

ACKNOWLEDGMENTS

This research was supported in part by Department of Energy Grant No. DE-FG03-87ER45324 and by INFM of Italy.

[1]B. I. Halperin, P. C. Hohenberg, and S. Ma, Phys. Rev. B **10**, 139 (1974).
[2]M. Marinelli, F. Mercuri, U. Zammit, R. Pizzoferrato, F. Scudieri, and D. Dadarlat, Phys. Rev. B **49**, 9523 (1994).
[3]M. Chirwa, L. Lundgren, P. Nordblad, and O. Beckman, J. Magn. Magn. Mater. **15-18**, 457 (1980); D. P. Belanger, P. Nordblad, A. R. King, J. Jaccarino, L. Lundgren, and O. Beckman, *ibid.* **31-34**, 1095 (1983).
[4]M. T. Hutchings, B. D. Rainford, and H. J. Guggenheim, J. Phys. C **3**, 307 (1970).
[5]D. P. Belanger and H. Yoshizawa, Phys. Rev. B **35**, 4823 (1987).
[6]G. K Wertheim and D. N. E. Buchanan, Phys. Rev. B **161**, 478 (1967).
[7]D. P. Belanger, Braz. J. Phys. **22**, 283 (1992).
[8]D. P. Belanger, B. Farago, V. Jaccarino, A. R. King, C. Lartigue, and F. Mezei, J. Phys. (Paris) Colloq. **49**, C8-1229 (1988).
[9]M. Chirtoc and G. Mihailescu, Phys. Rev. B **40**, 9606 (1989).
[10]M. Marinelli, U. Zammit, F. Mercuri, and R. Pizzoferrato, J. Appl. Phys. **72**, 1096 (1992).
[11]K. Hefner, Ph.D. thesis, University of Chicago, 1964.
[12]P. C. Hohenberg, A. Aharony, B. I. Halperin, and E. D. Siggia, Phys. Rev. B **7**, 2986 (1976).
[13]A. Aharony and G. Ahlers, Phys. Rev. Lett. **44**, 782 (1980).
[14]B. I. Halperin and P. C. Hohenberg, Phys. Rev. **177**, 952 (1969).
[15]P. C. Hohenberg and B. I. Halperin, Rev. Mod. Phys. **49**, 435 (1977).
[16]D. P. Belanger, A. R. King, I. B. Ferreira, and V. Jaccarino, Phys. Rev. B **37**, 226 (1987).